Energetic and exergetic performance assessment of the inclusion of phase change materials (PCM) in a solar distillation system

Mohamed S. Yousef[a,b,*], Hamdy Hassan[a,c]

[a] *Energy Resources Eng. Department, Egypt – Japan University of Science and Technology (E-JUST), Alexandria, Egypt*
[b] *Department of Mech. Eng., Benha Faculty of Engineering, Benha University, Benha, Egypt*
[c] *Department of Mech. Eng., Faculty of Engineering, Assiut University, Assiut, Egypt*

ABSTRACT

In this experimental work, the energetic and exergetic performance enhancement of solar distillation system (solar still incorporated with PCM storage unit) is performed by using two techniques. First, pin fins heat sink (PF) is embedded inside the PCM to act as a thermal conductivity enhancer. Second, black steel mesh fibers (SWF) are employed in the solar still basin with PCM. In this regard, four cases of the solar stills are studied and compared conventional still: conventional solar still (without PCM), still with PCM (With PCM), still with PCM and pin fins heat sink embedded in the PCM (With PCM-PF) and still with PCM and SWF in the basin (With PCM-SWF). The energetic and exergetic performance of the four cases is evaluated and compared under the meteorological conditions of New Borg El-Arab City, Egypt. The results show that the total daily cumulative yield of distilled water of still with PCM, still with PCM-PF, and still with PCM-SWF are greater than of conventional still by 9.5%, 16.8%, and 13%, respectively. Additionally, the inclusion of the fins heat sink in the PCM increases the average daily energy and exergy efficiencies by 17.9, and 13.2%, respectively compared to conventional one. Likewise, the energy and exergy efficiencies of still with PCM-PF are higher than those of solar still with PCM by 7.7 and, 6.8%, respectively. Furthermore, placing SWF in the basin of still with PCM significantly enhances the daytime energy and exergy efficiencies with a considerable reduction of these values in the nighttime. The total daily evaporative exergy for still with PCM-SWF is greater than those of conventional still, still with PCM, and still with PCM-PF by 13, 8, and 2%, respectively. Also, still with PCM, still with PCM-PF, and still with PCM-SWF exhibit an increment of the daily exergy efficiency 5.9, 13.2, and 17.3%, respectively compared to still without PCM. Still with PCM-PF achieved the highest accumulated daily water productivity and energy efficiency but still with PCM-SWF attained the highest daily exergy efficiency with nearly no additional cost.

1. Introduction

The accessibility of drinking healthy freshwater represents one of the main challenges facing the world these days, especially in remote and arid areas. Along with energy and food, drinking freshwater is one of the fundamental necessities for sustaining all life on earth. However, most of the available water is salty and isn't appropriate for drinking purposes, domestic use, industrial and agricultural needs [1,2]. It is noted that about 97% of available water on the surface of the Earth in seas and oceans is brackish water, while the remaining is freshwater rivers, lakes and frozen water locked up in polar ice regions and glaciers [3]. Industrialization of societies, unsustainable consumption rates, and the fast population growth cause unbalance between the increasing demand and the provision of freshwater. Therefore, to cover this severe shortage of freshwater and fulfill the high demand for freshwater, water

desalination is an obligatory solution [4]. A solar still is an inexpensive device that yields drinkable and potable water from salty water utilizing the energy from the sun. The basic phenomenon of this device is that brackish water lying inside a closed enclosure is evaporated using the trapped heat from the sun. Then, this water vapor is condensed on the glass walls of the still and then it is accumulated [5]. The simple type of solar stills is presently one of the best prevalent and commonly recognized designs for solar distillers. However, its low freshwater productivity is the main drawback which makes its real implementation limited [6]. Furthermore, the non-continuous operation of solar distillation systems due to uncertain availability and the intermittent nature of solar intensity is also one of the major defects, leading to a low yield of freshwater as compared to other desalination systems. These challenges affect the reliability of the solar desalination systems and hence, limit its implementation [7].

Numerous research works have been devoted to the enhancement of the solar stills' performance. Muftah et al. [8] and Rufuss et al. [9] conducted a review study to provide insights about the various methods and techniques employed to augment the yield of freshwater from the solar stills. They outlined that operational, and meteorological considerations such as wind velocity, location, environment temperature, solar intensity, the thickness of the covering surface, and water depth greatly affect the solar still performance. One of the common methods is the incorporation of solar collectors with solar stills [6]. Employing solar collectors boosts the average basin water temperature and thus, enhances the freshwater yield [10,11]. A theoretical investigation of the thermal efficiency of the addition of an evacuated tube collector with solar still is performed by Singh et al. [12]. It was reported that the maximum freshwater productivity and thermal efficiency are 3.8 kg/m^2 and 33%, respectively. The influence of using condenser in the form of the heat sink on the freshwater production of solar distillation unit was experimentally investigated by Hassan and Abo-Elfadl [13]. Their findings illustrated that the proposed system improved the daily yield of freshwater by 31%, compared to the traditional still. Coupling the photovoltaic thermal (PV/T) system with solar still is carried out by Pounraj et al. [14]. In this system, the saline water is heated before utilized in the solar still by using it in cooling the PV system. The proposed system improved the PV and solar still efficiencies by about 30, and 38%, respectively.

Additionally, using wicking materials and porous mediums in solar stills and other solar energy systems has received much attention in enhancing still productivity and performance. Using porous mediums in solar stills has several advantages over the conventional solar still [15]; (i) Wicking materials have the capillary action that produces large effective surfaces for convective and radiative energy transfers and consequently increases the evaporation surface. (ii) Due to its wick property, water can be transmitted through the evaporation surface more easily that results in more water can be exposed to the solar intensity and (iii) wicking materials are not expensive materials, making it very economical. However, the significant shortcoming of using such systems is that it has no nocturnal (overnight) water productivity like a conventional still without wicking materials [16]. Various designs of solar stills with different wicking materials are extensively investigated by large numbers of researchers [17–22].

Recently, employing thermal energy storage (TES) units with solar distillation systems seems to be an encouraging practical solution to solve the increasing imbalance between energy provision and energy consumption as a result of the intermittent nature of solar energy [23]. The advantage of using such systems is the storage of the extra heat in saline water during the daytime when the solar intensity is at peak periods (sunny hours) to be retrieved at nighttime during sunshine-off periods. Also, the TES units aid to decrease the heat dissipation from the absorber plate of the still by absorbing the lost heat during high solar radiation rates in the daytime [24]. TES systems are presently classified into two main forms viz., sensible and latent storage systems (LHS). Nevertheless, the LHS systems exhibit superior performance in comparison with the sensible storage one due to its excellent thermal storage capacity, isothermal phase change operation, and negligible volume changes during the melting and solidification phases [25]. Moreover, the application of latent heat storage (LHS) in the solar stills has recently gained much attention among researchers due to its promising features, as discussed earlier. In brief, El-Sebaii et al. [26] analyzed analytically the yield of simple type slope still in the presence and absence of PCM. Their findings indicated that as the amount of the PCM rises, the nighttime and total daily productivities also increase, while the daytime productivity decreases. In addition, the authors mentioned that shallow depths of brackish water in the basin result in higher freshwater yield in case of PCM is involved in the solar still. Dashtban and Tabrizi [27] examined the performance enhancement of a weir type solar desalination unit incorporated with a PCM storage unit under the basin. The findings revealed that the total freshwater

yield for a conventional still without PCM and a modified still with PCM are 5.2 and 6.8 kg/m^2 day respectively. Ansari et al. [28] theoretically investigate the freshwater yield enhancement of a passive solar desalination unit incorporated with PCM storage unit subjected to the climate environments of Morocco. The authors concluded that selecting the PCM material relies strictly on the peak temperature of saline water. The addition of a solar concentrator with a hemispherical solar still, in the presence and absence of PCM, is experimentally studied by Arunkumar et al. [29]. The experimental results indicated roughly 26% increment in the freshwater yield for the still with PCM related to a traditional one. Arunkumar and Kabeel [30] experimentally investigated the influence of the incorporation of PCM with a concentric circular tubular solar still (CCTSS) to improve the freshwater yield. The experiments were performed to study the effectiveness of using the CCTSS with and without PCM. The findings show that the freshwater yields, without and with PCM, are 5.3 kg/m^2/day and 5.8 kg/m^2/day, respectively, with an excess of about 8.4%. Al-harahsheh et al. [6] performed an experimental work to scrutinize the impact of incorporating a PCM storage unit on the freshwater yield of a solar still assisted by solar water collector. The findings exhibited that the output freshwater productivity is directly dependent on the hot water circulation flow rate. In addition, one of the outcomes is the inverse relationship between the saline water depth and water productivity, the productivity decreased as the water level increased.

Based on the previous advantages of using PCMs, a wide range of materials is tested as PCMs, including fatty acids, sugar alcohols, paraffin waxes, and salt hydrates, for the application of solar stills. Paraffin wax is considered the most used PCM material due to its promising features such as limited super-cooling, low cost, the great latent heat of fusion, chemically stable, and low vapor pressure. However, the inherently low thermal conductivity represents its major drawback. The poor thermal conductivity (roughly 0.24 W/m K) of PCM represents a key barrier for efficient thermal diffusion and overall heat transfer rates of energy dissipation during the melting and solidification phases [31]. To overcome this defect, various heat transfer augmentation techniques were developed. Some techniques include inserting extended surfaces such as microencapsulated PCM [32], nanoparticle additives [33], metallic foams [34], and mixing high conductive fillers with PCM [35]. Among all those above-mentioned methods, using extended fins and applying nanoparticles are the two most prevailing techniques to augment the heat transfer features in the PCM. However, employing PCM in a heat sink with finned configurations have been investigated extensively due to its ease of manufacture, simplicity, and cost-effectiveness. The insertion of highly conductive fins in PCM enclosures maximizes the projected area between the PCM and the basin liner, and thus boosts the rates of heat transfer and thermal diffusivity. Based on these advantages, several researches have inspected the effects of diverse fin configurations on the heat transfer features of the PCM in different applications, like solar water collector equipped with PCM with different number of fins fixed on the absorber plate [36], humidification-dehumidification system and solar air heater [37], helically coiled heat exchanger [38], cascade thermal energy storage [39], solar collector system [40], solar water collector with PCM [41], photovoltaic modules [42].

Lately, exergy evaluation approaches based on the second law of thermodynamics has gained significantly much attention among researchers for evaluating different energy systems performance, especially solar desalination systems. In comparison with energy methodology which is based on the first law of the thermodynamics, exergy analysis seems to be a prevailing perspective technique for the design, performance assessment, and optimization of energy systems. The energy analysis is only treated with the energy conservation principle, the quantitative aspect of the energy transfer, and provides no knowledge concerning the degradation of the system performance [1]. Conversely, exergy analysis provides an insight on the potential use of energy or the quality of energy and it is verified to be a compelling thermodynamic

tool to recognize the forms, real magnitudes, and locations of the losses and irreversibility in the system processes. This approach can be employed for designing, evaluating, and optimization of solar stills to minimize the origins of irreversibility, exergy destructions, and inefficiency in the prevailing mechanisms and processes of the solar desalination systems [43]. The exergetic performance of many solar distillation systems is rarely investigated in the literature [43–48]. In brief, Torchia- Nunez et al. [46] studied the exergetic assessment of simple type configuration. Their findings revealed that the exergy efficiencies of saline water, absorber plate, and the overall system are 6%, 12.9%, and 5%, respectively. Kianifar et al. [49] assessed the exergetic analysis of a pyramid-type solar still. The systems were evaluated in both passive and active modes by incorporating small fan (active mode) into the interior of the still to augment the evaporation rate. The findings indicated that the solar still in active mode showed superior exergetic performance compared to the still in passive mode. Asbik et al. [50] examined theoretically the exergetic performance of simple type solar still incorporated with PCM storage unit. The temperatures variations, freshwater productivity, exergy efficiency and irreversibility of the considered system are evaluated. The main outcome of the study is that although the freshwater yield increases due to using the proposed storage system, the exergy efficiency decreases. In another theoretical study, Sarhaddi et al. [51] presented a comparative exergetic analysis of two weir solar stills in the presence and absence of PCM storage unit under sunny and semi-cloudy meteorological circumstances. The simulation results revealed that solar still in the absence of PCM outperformed solar still in the presence of PCM concerning the energy and exergy efficiencies during sunny days. The comparative performance of double and single acting solar still incorporated with photovoltaic thermal compound parabolic concentrator concentrators based on the enviroeconomic and exergoeconomic analyses are performed by Singh and Tiwari [52]. The results revealed that freshwater productivity, overall efficiency, enviroeconomic and exergoeconomic parameters in case of double type solar still outperformed those of single type by 8.6%, 5.7%, 21.5%, and 16.2%, respectively.

The previous literature review confirms the significance of using PCMs in combination with the solar still to enhance the freshwater productivity, particularly at nighttime. In spite that large number of investigations have been performed on the performance of different solar still configurations with various PCMs, all these attempts are predominantly based on the separate investigation of energy performance, whereas a complete evaluation of the performance of these systems by considering the energy and exergy aspects, has received very little attention in literature. To the best of the author's knowledge, only two theoretical investigations conducted by Asbik et al. [50] and Sarhaddi et al. [51], who examined the exergetic performance of the addition of PCMs in simple type solar still and in weir type solar stills, respectively. However, the two above-mentioned studies showed some dissimilarity in the findings of the increase/reduction of the exergy efficiency due to using PCM storage unit with a solar still. Furthermore, Jegadheeswaran et al. [53] and Li [54] reported that the literature suffers a lack of studies regarding the promotion of exergy flux in PCM using different finned structures. Therefore, the performance, energetic and exergetic efficiencies of single slope solar still with PCM storage unit using two proposed techniques to augment these performances for the still with PCM are studied experimentally which haven't been considered previously. Firstly, pin fins heat sink is embedded inside the PCM to act as a thermal conductivity enhancing has not also studied before. Additionally, the exergetic performance of PCM with pin-finned heat sink for solar still applications hasn't been reported yet in the literature. Moreover, it is expected that during sunny hours, the daytime productivity of the solar still will be negatively affected due to using the PCM and thus the energy and exergy efficiencies will be adversely affected as well. Accordingly, this study stimulates us to use secondly black steel wool fibers (SWF) of higher thermal conductivity as a new porous medium in the still basin coupled with PCM unit which
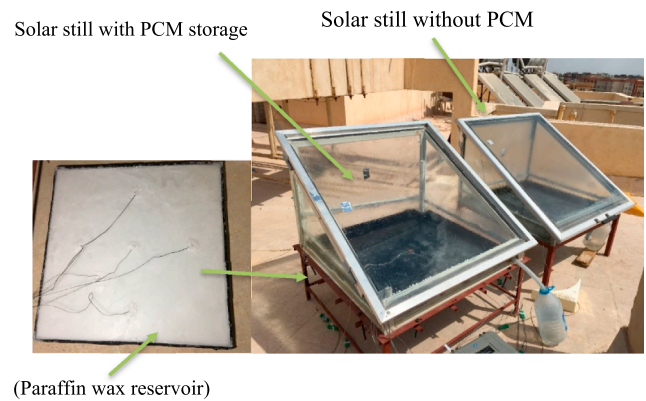

Solar still with PCM storage   Solar still without PCM

(Paraffin wax reservoir)

Fig. 1. A photographic of the experimental setup of the solar still with PCM.

hasn't been considered before in the literature. In this regard, four cases of solar stills are studied and compared namely, without PCM (conventional solar still), still with PCM, still with PF embedded in the PCM, and still with PCM and SWF in the still basin. The energetic and exergetic performance of the four cases is evaluated and compared to each other under the same atmospheric environments of New Borg El-Arab City, Egypt (Longitude/Latitude: E 029°42′/N 30°55′). Finally, a cost analysis is established to study the effectiveness of the all tested solar stills configurations economically.

2. Experimental work

2.1. Solar still design and construction

An experimental setup is established to examine the effect of incorporating PCM storage unit on the yield of freshwater, energy, and exergy performance of solar stills. A photograph of the experimental setup is displayed in Fig. 1. Two similar single slope passive solar stills of identical specifications and dimensions are tested and constructed at the same location for performance investigation and comparison, as indicated in Fig. 1. The absorber liner of each solar still has a projected area of 1 m², whereas the elevations of the front and back walls are 12 cm and 70 cm, respectively. The basin liner is fabricated from galvanized iron with a thickness of 4 mm and it painted with a black material at its base to maximize the solar intensity capturing. Armaflex insulation was used as a thermal insulator for both stills to prevent the dissipating heat from the basin liner to the atmosphere and to the base in case of still without PCM. The entire solar still (top cover and lateral walls) are fabricated from a transparent glass with a thickness of 5 mm. A rubber gasket is employed for the sealing between the solar still edges and the glass cover to prevent any vapor leakage and to makes it airtight. The two solar stills are positioned on the East-West axis, fixed in the south direction, and the slope of the condensing glass is adapted to be equal the latitude of the place to accumulate the maximum amount of incident solar intensity. Three small channels are welded along both inner sides of the solar still with 5 degrees' downward inclination. Due to its tendency, the condensate water could be easily accumulated and glided downward through these channels to be collected in 6 L bottle and then measured by using a calibrated flask.

For the solar still with PCM, a heat reservoir, made of galvanized steel, with a thickness of 26 mm is placed beneath the basin line of the solar still and it is fully packed by the paraffin wax that functions as a thermal energy storage unit, as depicted in Fig. 1. Based on the size of the PCM reservoir, the used mass of the PCM is 15 kg of paraffin wax weighted by using a calibrated balance. It is worth mentioning that the volume of the paraffin wax is predicted to be expanded by 12% of its volume due to its phase changing from solid phase to liquid phase. Thus, 2 kg of paraffin wax as excess volume was added to make sure that the area of contact between the PCM and the basin liner is perfect.

This is essential to enlarge the heat exchange between the PCM and the basin liner. Therefore, 17 kg as a total weight of wax is employed to occupy the PCM reservoir. The PCM reservoir is properly insulated using Armaflex insulation sheet to minimize heat dissipation from its sides to the atmosphere. The PCM tank is designed in a way to make sure that a good contact will be achieved with the bottom surface of the basin liner. The rubber gasket is used for sealing between the PCM reservoir edges and the bottom surface of the absorber plate to prevent any leakage. In case of using PCM, the heat is lost from the saline water through the basin base by conduction and stored inside PCM at daytime and then it returns to the saline water as will be explained later. In case of still without PCM, the basin base is insulated as stated previously to minimize the heat loss from the basin base to the ambient.

In this setup, two techniques are proposed to augment the energetic and exergetic performance of solar distillation with PCM. In the first set of the experiment, the heat transfer features of the PCM storage unit, applicable to solar still system, is enhanced by utilizing hollow cylindrical pin fins embedded in the PCM. Hollow cylindrical pin fins are used because they occupy smaller volume compared to the total PCM volume and also, they act as heat transfer enhancer because they have higher heat transfer surface area between the fins and the PCM and maximize the projected surface area between the PCM and basin liner resulting an increase of the heat transfer inside the PCM and thus augments the rates of storing and retrieving energy/exergy transfer from and to the saline water. In this setup, paraffin wax is chosen as a PCM material because of its favorable features such as low cost, non-toxicity, the large latent heat of fusion, uniform melting, safety, and reliability. In our study, the selection of the type of the PCM rest on the properties and the characteristics of the operating conditions. Thus, the melting point of the selected PCM is 56 °C, which is appropriate for our working conditions and environmental parameters. The thermo-physical characteristics of paraffin wax employed in this study are tabulated in Table 1. Fig. 2 exhibits the schematic diagram of the solar distillation system with the PCM-based pin-finned heat sink in which all parts of the system are highlighted. A heat sink consists of 225 (15 × 15) hollow cylindrical PF with dimensions of (19 mm outside diameter, 1 mm thickness, and 26 mm long). The pitch between each two consecutive pin fins is taken as 5 cm. All these PF are fastened onto the rear surface of the basin liner and are arranged in inline distribution, as shown in Fig. 2. These fins constitute approximately 4% of the overall volume of the heat sink. The extended fins are employed to augment the contacting surface area between the basin liner and the PCM and consequently, they enhance the heat transfer rates. The fins are made of copper material due to its higher thermal conductivity.

It is expected that during sunny hours, the daytime productivity of the solar still will be negatively affected due to using the PCM and thus the energy and exergy efficiencies will be adversely affected as well. Thus, another set of experiments is performed to examine the effect of using SWF as a new porous medium at the basin of the solar still with PCM on the daytime performance of the still, as shown in Fig. 3. This is to compensate for the loss in evaporation of the saline water during the daytime due to the heat transported to the PCM from water. The idea behind using this material is the wicking property that produces large effective surfaces for convective and radiative energy transfers and consequently increasing the evaporation surface. Using SWF as a porous medium has many advantages over other previously studied materials

in literature. (i) SWF have relatively high thermal conductivity [56] which means a higher heat transfer rate inside the saline water resulting in an increase in water temperature. (ii) They produce large effective surfaces for convective and radiative energy transfers and consequently increasing the evaporation surface, and (iii) SWF are very cheap and easily accessible in local markets. One kg of steel wool fibers weighted by using a calibrated balance is completely distributed in the basin and fully immersed into the brackish water and as result of the capillary action of steel fibers, water moves up through its fine threads, resulting in the large surface for evaporation. Moreover, because of the higher thermal conductivity of the SWF, the heat transfer within the saline water will be increased. In this regard, four cases are studied and compared namely; solar still without PCM (without PCM), still with PCM (with PCM), still with PF embedded in the PCM (with PCM-PF), and solar still with PCM and SWF in the basin (with PCM-SWF). The energetic and exergetic performance of the four cases is experimentally evaluated and compared to each other under the same meteorological environments of New Borg El-Arab City, Egypt (Longitude/Latitude: E 029°42′/N 30°55′).

2.2. Measurements

A pyranometer was mounted alongside the experimental set-up to measure the incident solar intensity at a horizontal level. The depth of saline water for both solar stills remains constant at 1.5 cm during all the tests. The water used in the experimental work is seawater from the Mediterranean Sea with an initial PH value of 8.44–8.53 and total dissolved solids (TDS) value of 25–30 g/l [57,58] and the desalinated water PH is 6.4 which inside the limit of drinking water. Calibrated thermocouples of Type K are used to measure the temperatures of diverse sections of each solar distillation system, viz. inner and outer glass covers, back cover, basin liner, saline water, humid air, PCM, and ambient temperature. The temperature of PCM is calculated using the average reading of six thermocouples distributed in six different locations and at different depths in the PCM reservoir. One thermocouple is attached at the center of the basin liner to measure its temperature. Another thermocouple was employed to measure the temperature of the salty water. The inner and outer glass temperatures are also recorded by using two other thermocouples. During each test, the distillate freshwater is measured periodically every one hour using a calibrated flask with a capacity of six liters. A meteorological weather station is used to measure the wind velocity. The humid air temperature is also recorded using another sensor. Also, a thermocouple is attached to the back side of the solar still. All attached thermocouples are linked to a data logger and all measured data are recorded on an hourly basis. Monitoring the energy charging and discharging periods is essential to assess the physical phenomenon of the PCM. For this purpose, the measurements are recorded every hour for a full-day cycle starting from 7:00 AM until the time 3:00 AM in the next day. All experiments of both sets are conducted on three convergent days from 2 September 2017 to 5 September 2017 to ensure that the solar intensity variation during the reading days doesn't change much as will be shown later to decrease the effect on the results during the comparison. It is also noted that the wind velocity doesn't change much during the reading days as stated in Table 2 where the maximum variation with the average wind velocity during the measuring days is about 0.18 m/s as also illustrated in Table 2.

2.3. Experimental procedure

The experimental work procedures are carried out as the following procedures in order:

1- Before doing any experimental measurements, the experiment is prepared carefully where the hours before starting the reading, the water is supplied to the basin and its quantity and level are checked

Table 1
Thermophysical characteristics of the used PCM [55].

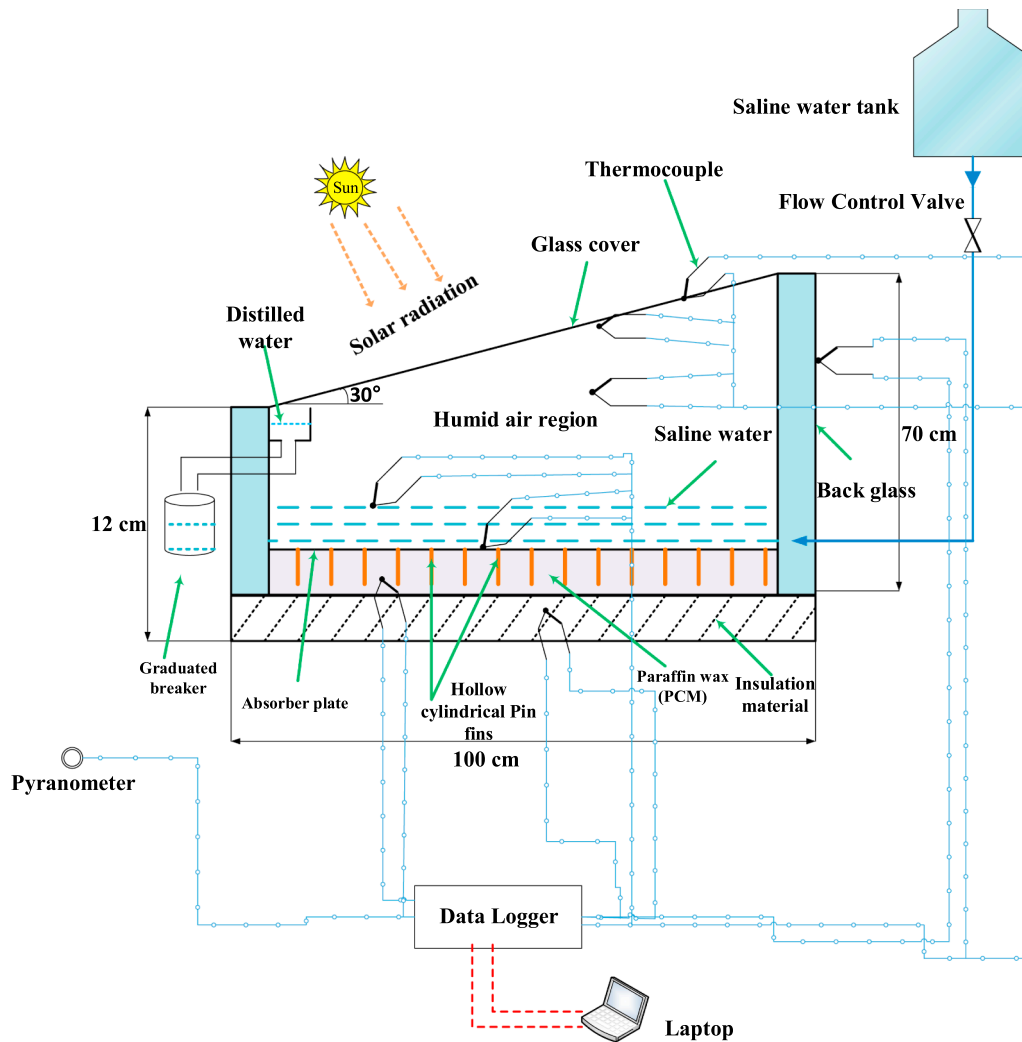| Property	Value
Melting temperature	56–58 °C
Density of liquid/solid	760/818 kg/m^3
Specific heat of liquid/solid	2510/2950 J/kg °C
Latent heat of fusion	226000 J/kg
Thermal conductivity of liquid/solid	0.24/0.24 W/m °C

Fig. 2. Schematic diagram of the single type solar distillation with PCM-based pin fin heat sink.

carefully. Also, checking the PCM quantity, measuring instruments, al system insulations, SWF quantity, PF fastening, etc. depending on each studied case.

2- During each time measurements, ensuring that taking the measurements at the same time and be sure that the temperature logger registers the reading values, Pyranometer records solar energy, meteorological weather station records the wind velocity, etc.

3- The collected yield freshwater quantity is measured carefully and registered.

4- Repeat the previous two procedures (3 and 4) each time step reading.

5- At the end of all-day readings, preparing the solar still system as the first reading day (ensure that the glass cover is clean, all insulated system parts are well insulated to prevent leakage, etc.), and then do

Fig. 3. A photographic of the setup of the solar still with PCM and steel wool fibers.

Table 2
Measured wind velocity in m/s throughout the measuring days.

Time	2 Sept. 2017	4 Sept. 2017	5 Sept. 2017
7:00	1.5	1.4	1.23
9:00	1.2	0.9	0.87
11:00	3.24	3.35	3.29
13:00	3.36	3.1	2.97
15:00	2.85	3.31	4
17:00	2.61	2.6	2.43
19:00	2.96	2.65	2.22
21:00	3.68	2.87	2.6
Average	2.7	2.32	2.6

the procedure 1 to do the next day readings.

2.4. Uncertainty and error analysis

In this study, the uncertainties arising from instruments during the experimental measurements are studied. Some of these values are taken from the instruments data sheet and other values are obtained by the instrument supplier. The uncertainties and errors of the experimental results are computed based on the methods presented by Taylor [59]. The uncertainties of directly measured variables such as temperature and productivity consider the sources of errors, random and systematic. The uncertainty δ of value f such as still efficiency computed from the experimental results is computed based on the following equation [59].

$$\delta = \sqrt{\left(\frac{\partial f}{\partial x}\right)^2 \delta_x^2 + \left(\frac{\partial f}{\partial y}\right)^2 \delta_y^2} \tag{1}$$

where δ1 and δ2 are the uncertainty of measured values x and y, respectively and this equation can be applied to more than two measured values. Based on this equation, the uncertainty of the efficiency is found to be 1.9%. The uncertainties of the measured values are illustrated in Table 3.

3. Theoretical background analysis

3.1. Energy analysis

For more analyzing and interpreting the results, the thermal efficiency of the solar still is calculated for all considered cases. The daily energy efficiency of the solar still is estimated by using the next formula [13,55].

$$\eta_{th} = \frac{P_d \times L_{av}}{A_p \times I_d} \tag{2}$$

where Pd is the total daily freshwater productivity in kg, Lav is the latent heat of evaporation of water in J/kg, Ap is the projected area of the solar still in m^2, Id is overall daily of the incident solar energy on the solar still in J/m^2.

3.2. Exergy analysis

Exergy analysis function represents an indicator of the capability of energy to do work and it is formulated from the second law of

Table 3
The uncertainties and accuracy values of the measuring instruments.

Instrument	Accuracy	Measuring range	Uncertainty
Thermocouple	± 0.1 °C	0–1260 °C	0.074 °C
Pyranometer	± 10 W/m^2	0–1500 W/m^2	0.841 W/m^2
Meteorological weather station	± 2%	1–150 m/s	0.01 m/s
Measuring beaker	± 0.01 ml	0–6000 ml	5×10^{-5} ml
Data-logger	± 0.1 °C	0–1000 °C	0.1 °C

thermodynamics. Exergy is termed as the utmost amount of work that can be attained from a given system as it reaches to thermodynamic equilibrium in a specified environment. The following equation describes the general form of the exergy balance [60]:

$$\sum \dot{E}_{x,in} - \sum \dot{E}_{x,out} = \sum \dot{E}_{x,dest} \tag{3}$$

The exergy input to the solar still is the solar irradiance exergy and is estimated by [60]:

$$\dot{E}_{x,in} = \dot{E}_{x,sun} = A_b I_t \left[1 - \frac{4}{3}\left(\frac{T_{amb} + 273}{T_s}\right) + \frac{1}{3}\left(\frac{T_{amb} + 273}{T_s}\right)^4 \right] \tag{4}$$

where A_b is the effective area of the still basin in m^2, I_t is the accumulated solar irradiance incident on the solar still in W/m^2, T_s is the sun temperature, 6000 K, and $\dot{E}_{x,sun}$ is the exergy input to the solar still from the solar insolation.

Exergy output of the product (distillate water) for a defined solar still can be given by [48,61]:

$$\dot{E}_{x,out} = \dot{E}_{x,evap} = \frac{\dot{m}_{ew}\lambda_{fg}}{3600}\left[1 - \left(\frac{T_{amb} + 273}{T_w + 273}\right)\right] \tag{5}$$

where $\dot{E}_{x,evap}$ is the output evaporative exergy and λ_{fg} is the latent heat of vaporization.

$$\lambda_{fg} = 3.1615 \ (10^6 - 761.6*T_i), \quad T_i > 70 \tag{6}$$

$$\lambda_{fg} = 2.4935 \begin{pmatrix} 10^6 - 947.79 \times T_i + 0.13132 \times T_i^2 \\ - 0.0047974 \times T_i^3 \end{pmatrix}, \quad T_i < 70 \tag{7}$$

where $T_i = \frac{T_w + T_g}{2}$ and L$_{av}$ is assumed that equals λ_{fg}.

The exergy efficiency can be computed as the ratio between the desired output exergy and the input exergy and it is expressed as [46].

$$\eta_{ex} = \frac{\dot{E}_{x,out}}{\dot{E}_{x,in}} = \frac{\dot{E}_{x,evap}}{\dot{E}_{x,in}} \tag{8}$$

3.3. Economic analysis

The main target of any solar still system it to cut down the cost of production per liter (CPL) of distillate water. The studied cases are economically examined and the economic analysis procedures can be shortened as follows [62]:

The first annual cost (FAC) of a solar distillation unit is given by [63]:

$$FAC = CRF \times P \tag{9}$$

where P and CRF represent the capital cost of the solar still and the capital recovery factor, respectively.

The Capital Recovery Factor (CRF) is computed as [13,63]:

$$CRF = \frac{i(1 + i)^n}{(1 + i)^n - 1} \tag{10}$$

where i denotes the annual rate of interest and n denotes the lifetime years of the solar still which is assumed to be ten years [13].

The annual salvage value (ASV) of the solar distillation unit is given by [63]:

$$ASV = SSF \times S \tag{11}$$

where SSF and S represent the sinking fund factor (SFF) for a system and the salvage value of the solar still, respectively.

S is given by [63]:

$$S = 0.2 \times P \tag{12}$$

SSF is given by [63]:

$$SSF = \frac{i}{(1 + i)^n - 1} \tag{1}$$

The maintenance cost (AMC) per year is supposed 15% of the first annual cost [63]:

$$AMC = 0.15 \times FAC \qquad (2)$$

The whole annual cost of the solar distillation unit is given by [63]:

$$AC = FAC + AMC - ASV \qquad (3)$$

Lastly, the cost per liter (CPL) of the freshwater yield is determined by [63]:

$$CPL = \frac{AC}{P_n} \qquad (4)$$

where P_n represents the average annual distilled water production.

4. Results and discussions

In this work, the energy and exergy analysis of the simple type solar distillation unit with PCM is experimentally presented. Two heat transfer enhancement systems are performed for the solar still with the PCM; (i) enhancement of the heat transfer inside the PCM by using PF and (ii) enhancement of the heat transfer inside the basin by employing steel wool fibers. Using pin fins heat sink inside the PCM increases the heat transfer from the basin to the PCM especially during the first half of the day which has a negative consequence on the evaporation of the daily saline water and a positive consequence on the stored energy inside the PCM during the daytime to be used during the last day and night times. Moreover, using pin fins inside the PCM enhances the releasing of the stored energy in the PCM to the brackish water during the nighttime (positive effect on the solar still performance). Contrarily, using SWF at the basin augments the daily evaporation of the saline water because of their higher thermal conductivity (positive effect on the evaporation). But, it decreases the lost energy to the PCM due to enhancing the evaporation rate (negative effect). The performance of the all tested cases is compared based on the solar still temperatures, productivity, energy efficiency, exergy efficiency, and cost per liter.

4.1. Solar still temperatures

Studying the evolution of the temperatures of each part of the solar still with time gives a good indication of the still operation and performance and helps to interpret the still produce results. The evaporation of the salty water is enhanced with the escalation of the water temperature and the temperature difference between humid air and water. While the condensation of the evaporated water enhances with the increment of the difference between humid air and glass temperature [3,13]. Fig. 4 presents the temperatures variations of inner glass cover (T_{ig}), humid air (T_{ha}), saline water (T_w) and absorber plate (T_p) with time for solar still without PCM (case1: conventional case). The
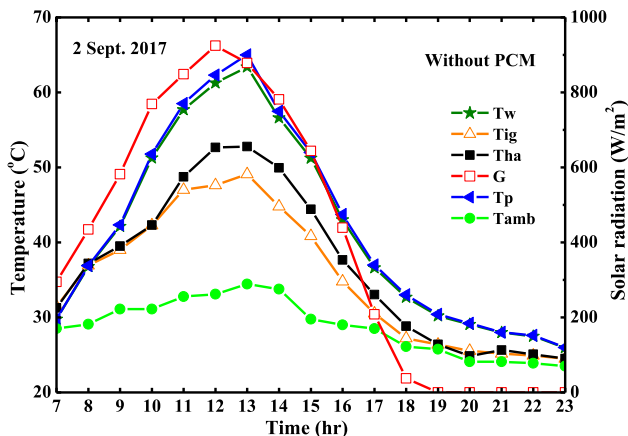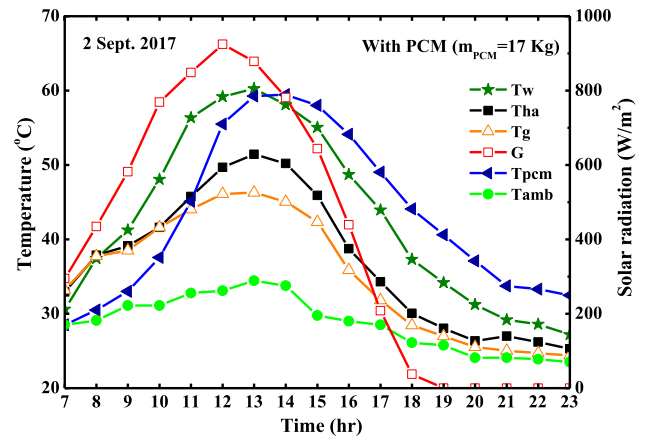
Fig. 5. Temperatures evolution with time for the solar still with PCM.

measured ambient temperature (T_{amb}) and solar radiation (G) are also superimposed on this figure. As seen, as the time progresses, all temperatures show an upward trend until they have peak values at around 13:00 PM then, they gradually decline until sunset. Moreover, the glass temperature is marginally larger than the brackish water temperature during the early hours in the morning. This result is credited to the heat capacity difference between glass and water and the time taken by the glass to be heated up before heating the water. Then, the water temperature shows a faster increase in its temperature compared to the glass temperature because of the heat dissipation from the glass to the environment and the heat gain absorbed by the saline water. The maximum temperatures of the inner glass cover, humid air, brackish water, and absorber plate are 49 °C, 52.8 °C, 62.4 °C and 64 °C, respectively. Additionally, the peak values of the measured ambient temperature and the solar intensity are 34.5 °C and 924 W/m², respectively. Fig. 5 illustrates the same previous parameters of Fig. 4 but for still with PCM. As seen also from Fig. 5, when the time increases, all temperatures increase gradually until they reach peak values at around noontime and after that, they steadily decline until the end of the day. Additionally, it is noticed that the maximum temperature of inner covering glass, humid air, brackish water, and the ambient temperature is 46.3 °C, 51.3 °C, 60.5 °C, and 34.5 °C, respectively and the peak value of the solar insolation is 924 W/m². In the beginning, the PCM temperature increases progressively with the time because it receives thermal heat from the basin. Firstly, the absorbed thermal energy from the basin stored initially as a sensible heat in the solid PCM until its temperature reaches the melting point (ranges from 56 to 58 °C). Then, the temperature of PCM remains constant for a while, indicating the solid-liquid phase changing process (melting process). Fig. 5 indicates that the complete melting of the PCM is achieved when the paraffin wax temperature (59.3 °C) exceeds the melting point range at about 14:00 PM. After 14:00 PM, the discharging process starts and the PCM temperature is kept constant until the PCM totally solidifies and afterward its temperature declines steadily until the end of the day. This is due to the losing heat from the PCM to the saline water and it is completely melted. It is also perceived that during the nighttime, the PCM temperature is continuously larger than the brackish water temperature because of the stored energy in the PCM at the daytime. This indicates that the discharging process continues at the night. Moreover, the water temperature of the solar still with PCM is kept warmer for a long time compared to the still without PCM (see Fig. 4). It is also noted that the coupling of the PCM storage systems with the solar stills, extends the still operation time after sunset for still with PCM by about 6 h because the still temperatures remain hotter for a longer time than conventional still. Figs. 4 and 5 depict that the water temperature is bigger than the humid air temperature and the latter is higher than glass temperature and the effect of this relations will be discussed later.
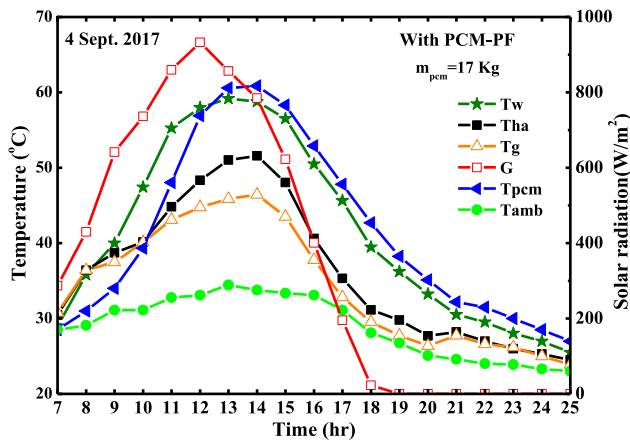
Fig. 4. Temperatures evolution with time for the still without PCM.

Fig. 6. Temperatures evolution of the solar still with time for solar still with PCM-PF.

Fig. 7. Temperatures distributions for solar still with PCM and SWF.

Fig. 8. Temperatures variations of humid air and water with time for the studied cases.

The same previous results in Figs. 4 and 5 but for still with PCM and PF integrated inside the PCM (With PCM-PF) are shown in Fig. 6. For about the same trend of Figs. 4 and 5, Fig. 6 indicates that the still temperatures rise steadily for the first half of the day and then they decline to the end of the day following the trend of incident solar radiation on the still. Also, it is noted that still with PCM-PF has the same trend stated previously of the relation between the brackish water, humid air and glass temperature of conventional still and still with PCM. For still with PCM-PF, it is observed that the maximum temperature of the inner glass cover, humid air, saline water, ambient air is 45.3 °C, 50.2 °C, 59.1 °C, and 34.8 respectively and the peak value of the solar intensity is 932 W/m². Still with PCM-PF shows that the maximum value of the PCM temperature is 60.85 which means complete melting of the wax material. Additionally, Fig. 6 reveals that the temperature of the PCM displays nearly a flat trend during the period from 13:00 to 14:00 which indicates the phase change time from solid to liquid of the PCM material during the charging process. Also, this figure indicates that the water temperature is kept warmer for long period after sunset compared to previously states presented in Figs. 4 and 5. Moreover, Figs. 4 and 5 illustrates that the temperature of PCM in case of still with PCM is higher than the PCM temperature in case of still with PCM-PF at the end of the day. This is due to including fins inside the PCM accelerates the energy loss from PCM to water resulting in a decrease of the PCM temperature. It can be concluded that inclusion of the PCM in the application of solar stills, extends the operation time after sunset for still with PCM-PF by 8 h compared to 6 h in case of still with PCM.

As shown in Figs. 5 and 6, the evaporation of the brackish water of the solar distillation systems with PCM and with PCM-PF, during the daytime hours, is significantly dropped because of decreasing water temperature which has an adverse impact on the still productivity. Therefore, a modification is carried out in the still to boost the evaporation of the solar still with PCM by using SWF in the basin of the solar still. As stated previously, SWF act as a porous medium which can enhance the convective energy and evaporative energy during the sunshine hours. Accordingly, another case is considered; still with PCM-SWF. The temperature variations for still with PCM-SWF of the inner glass cover, humid air, saline water, and PCM, ambient air and solar intensity with time is presented in Fig. 7. As perceived from Fig. 7, as the day progresses, all temperatures increase gradually until they reach a maximum value at midday and afterward they steadily decline until the end of the day which follows the incident solar energy power. It is noticed that the peak temperature of the inner glass cover, humid air, brackish water, and ambient air is 50 °C, 56 °C, 63 °C, and 33.6 °C respectively and the peak value of the solar insolation is 917 W/m². Additionally, the maximum value of the PCM temperature is 60.5 which means complete melting of the wax material. It can be observed from
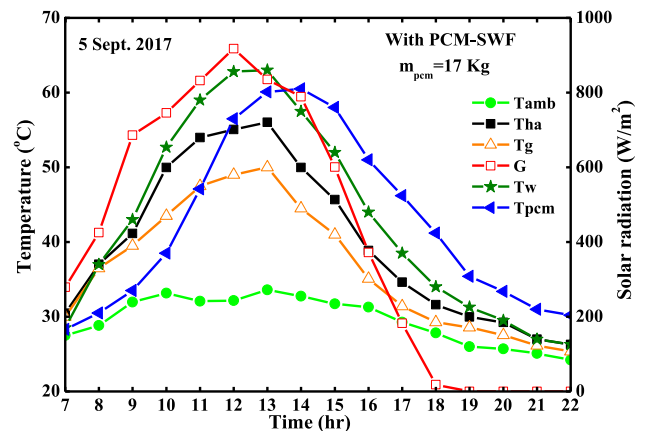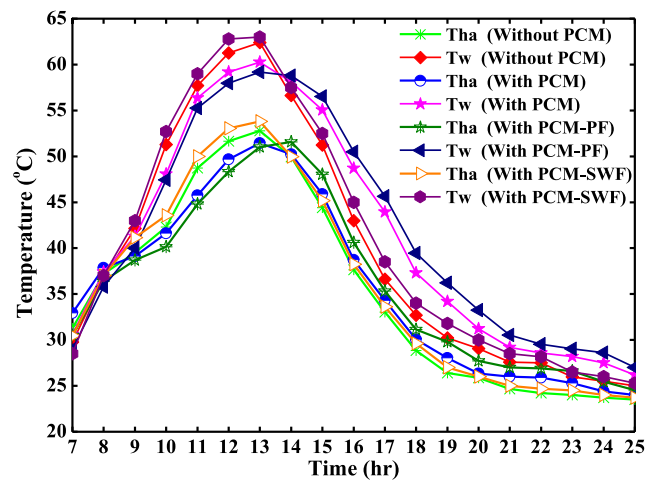
the graph that using PCM in case extends the still operation time after sunset by about 5 h.

As stated, the evaporation process increases with raising the temperature difference between the saline water and humid air. Fig. 8 presents the variations of humid air and water temperatures for the four previous cases. The figure exhibits that the brackish water temperature is larger than the humid air temperature throughout the day which indicates the evaporation of the brackish water, as stated previously. The findings also indicate that from the morning to the timing of about 13:00 PM, the temperatures of the humid air and brackish water in conventional still are greater than the corresponding values in still with PCM and still with PCM-PF because of the energy lost to the PCM in case of stills with PVM. Moreover, the temperatures of humid air and brackish water in still with PCM are greater than the corresponding values in still with PCM-PF because the PF increases the heat transfer from the basin to PCM in the morning and contrarily at the end of the day as will be shown later. From 13:00 pm onwards, this figure displays opposite trends where the humid air and brackish water temperatures in still with PCM-PF become the maximum, while those in the conventional still become the least and those in the still with PCM are intermediate. Such findings can be clarified as follows; during first daytime hours, the charging process of phase change materials starts by absorbing thermal energy from saline water. Therefore, a reduction in humid air and saline water temperatures is observed in case of still with PCM and still with PCM-PF than those in conventional still. Also, embedded the PF inside the PCM increases the heat transfer from the briny water to the PCM during the charging process, therefore at this period,

the temperature of still with PCM-PF is lower than still without PCM. After 13:00 PM, the discharging process of the PCM starts by releasing the stored thermal energy in PCM to saline water which explains that the humid air and brackish water temperatures in cases still with PCM and with PCM-PF are greater than the corresponding values in conventional still and still with PCM-PF is greater than still with PCM. This is due to as stated previously after 13:00 PM, the released heat from the PCM to the salty water yielding that the temperature of still with PCM is greater than conventional still and the positive influence of the pin fin heat sink on the discharged heat in still with PCM-PF yielding a higher temperature of still with PCM-PF than with PCM only. Fig. 8 reveals that during the charging phase, the temperature difference between the brackish water and humid air is greatest in conventional still and is smallest in still with PCM-PF where the largest temperature difference between the brackish water and humid air is approximately 9.6, 9.2 and 8.9 for conventional, with PCM, and with PCM-PF, respectively. These findings signify that the evaporation rate in still without PCM is greater than still with PCM and the latter is greater than still with PCM-PF during this period. This reveals that the expected daytime productivity of conventional still will be higher than still with PCM and the productivity of this case will be greater than still with PCM-PF as will be shown later. Another important observation from Fig. 8 is that during the daytime hours before noontime, the humid air and brackish water temperatures for case 4 exceeds than those of still with PCM and still with PCM-PF, whereas the corresponding values in case 4 becomes lower in the second half of the day. Such a trend can be attributed to the enhanced convective and evaporative energy transferred due to placing SWF in the basin in still with PCM-SWF, from the morning to the timing of 13:00 PM. This will result in a rise in the water temperature and more absorbed heat by the Paraffin wax, compared to still with PCM and still with PCM-PF. On the contrary, after noontime during the end times of the day, the humid air and brackish water temperatures values in still with PCM-SWF are lower than the corresponding values of still with PCM and with PCM-PF. This trend can be credited to the evaporation process of the salty water with the time. The evaporation of the brackish water makes that the upper layers of the SWF are not saturated well with the brackish water as the initial times resulting in a decrease of the evaporation rate with time and a decrease in the humid air temperature.

4.2. Freshwater productivity

The main target of the solar still is the production of freshwater. Therefore, it is essential to explore the consequence of the previous techniques (using pin fins heat sink inside PCM and using SWF at the basin with PCM) on the yield of the solar still. Figs. 9 and 10 display the variations of the freshwater yield for the studied stills with time. Fig. 9 presents the hourly values of the freshwater productivities and Fig. 10 illustrates the values of the total accumulated water productivity for the four previous cases. As seen in Fig. 9, for all the considered cases, the hourly freshwater productivities values increase gradually from the starting of the day at 7:00 AM until they reach peak values at time from 13:00 PM to 14:00 PM (approximately one hour later of the time of maximum solar intensity due to the shift time between the incident solar energy and the heating of the brackish water) and then, they decline until the end of the day. Fig. 9 illustrates that the hourly water productivity values before about 14:00 PM in conventional still is greater than the corresponding values of still with PCM and still with PCM-PF due to the lost heat energy to the PCM in these cases as explained previously. After that time, the hourly freshwater productivity for still with PCM and still with PCM-PF is greater than conventional still because of the gained heat energy from the PCM. Another important observation is that, during the morning and before about 1:00 PM, still with PCM-SWF has the highest productivity because of the higher water temperature and the temperature difference between the humid air and the water resulting in a higher water evaporation as
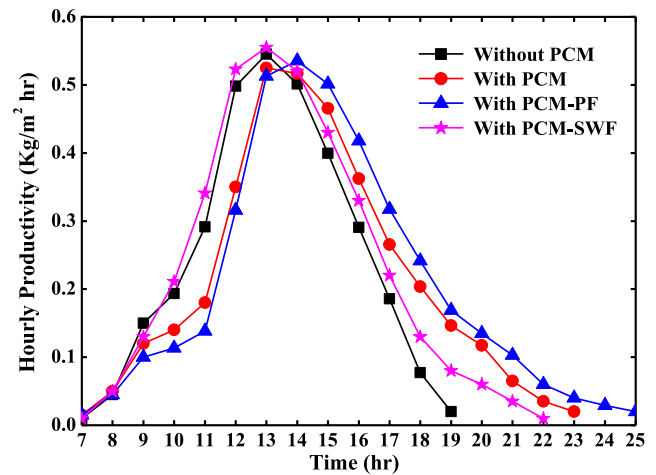

Fig. 9. The rate of hourly freshwater productivity with time for the studied cases.
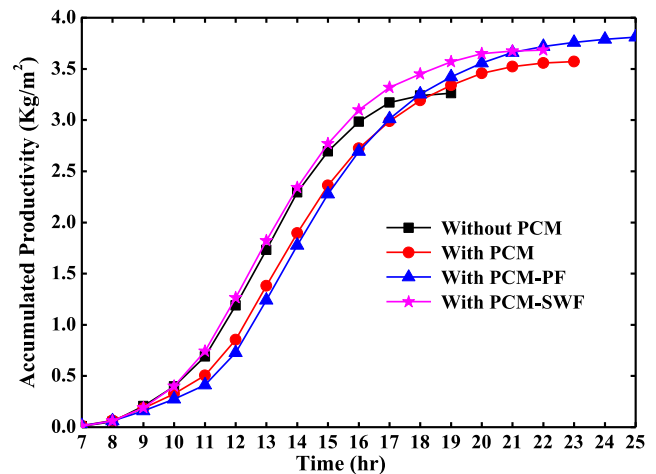

Fig. 10. Accumulated freshwater productivity with time for the studied cases.

stated earlier. However, during the nighttime, the hourly water productivity values in still with PCM-SWF is lower than the corresponding values of still with PCM and still with PCM-PF. This trend is due to the decrease in the evaporation of the saline water with advancing the time as explained previously. In Fig. 10, during the daytime, from 07:00 AM to 13:00 PM, the total accumulated freshwater yield for conventional still is greater than corresponding values in still with PCM and still with PCM-PF by approximately 7% and 11%, respectively. The reason for this result is that in conventional still, during this period, the absorbed solar energy is completely utilized for water evaporation which maintains water temperature at higher values as stated previously. Whereas in still with PCM and still with PCM-PF, the absorbed solar energy by saline water is reduced due to the dissipation of the thermal energy from brackish water to the PCM. During the nighttime, solar still without PCM yields very limited productivity (one hour after sunset); however, in case of the still with PCM and with PCM-PF, the distillation process continues because of the discharging energy from the PCM to the salty water. Furthermore, the results in Fig. 10 illustrate that during the daytime period from 10:00 AM to 13:00 PM, the total daytime freshwater yield for still with PCM-SWF is greater than the corresponding values in conventional still, still with PCM, and still with PCM-PF by approximately 7, 14, and 18%, respectively. This is as a consequence of the higher water temperature and temperature difference in the saline water and humid air in still with PCM-SWF than still with PCM and still with PCM-PF at this period as indicated before. It is also noted that for the same reasons of the previous result, the total

daily accumulated water productivity of still with PCM-SWF is greater than with PCM. This means that the positive effect of using SWF with PCM is the dominant compared to the positive effect of using PCM. The results revealed that the total accumulative freshwater yields, for conventional still, still with PCM, still with PCM-PF, and still with PCM-SWF are approximately 3.26, 3.572, 3.81, and 3.685 kg/m², respectively. Furthermore, the findings revealed that the total daily accumulative freshwater yield of still with PCM-PF is higher than those of conventional still, still with PCM, and still with PCM-SWF by around 16.7, 6.6, and 3.4%, respectively. This finding indicates that the integration of the extended fins in PCM is more effective than using SWF inside the still basin and the later affects positively on the productivity of the still with the PCM. One further observation is that the inconsiderable difference in hourly freshwater yield between still with PCM and still with PCM-PF is observed, at noontime from 13:00 PM to 14:00 PM, where the melting process of PCM in both cases takes place. However, from 14:00 PM onwards, still with PCM-PF yields the highest water productivity compared to other cases. Moreover, it is perceived that the total daily freshwater productivity of still with PCM is greater than that of conventional still by about 10%; whereas the total daily freshwater productivity values in still with PCM-SWF is greater than the corresponding values in still with PCM and conventional still by about 7% and 13%, respectively because of the positive effect due to using SWF inside the still basin. Figs. 9 and 10 illustrate that the integration of the PCM storage systems extends the distillation time after sunset for still with PCM, still with PCM-PF and still with PCM-SWF by approximately 5, 7, and 4 h, respectively. To conclude, integrating SWF with PCM is effective in enhancing the overall productivity of the solar still related to solar still with PCM but is less effective in comparison with solar still with PF, which achieved the highest freshwater productivity.

4.3. Energy and exergy efficiencies

Fig. 11 displays the hourly evolution of instantaneous energy efficiency with time for the four tested cases. As seen, as the time passes, all energy efficiencies rise progressively until they reach a maximum value at midday for conventional still and nearly 19:00 PM for cases (still with PCM, still with PCM-PF, and still with PCM-SWF) and then they decline steadily until the end of the day. The results exhibit that the maximum energy efficiencies of conventional still, still with PCM, still with PCM-PF, and still with PCM-SWF are approximately 42, 75, 83, and 64%, respectively. Furthermore, it was observed that the addition of PCM system (with PCM), with PCM-PF, and with PCM- SWF enhances the average daily energy efficiency by 9.4, 18 and 16%, respectively, in comparison with the conventional still.

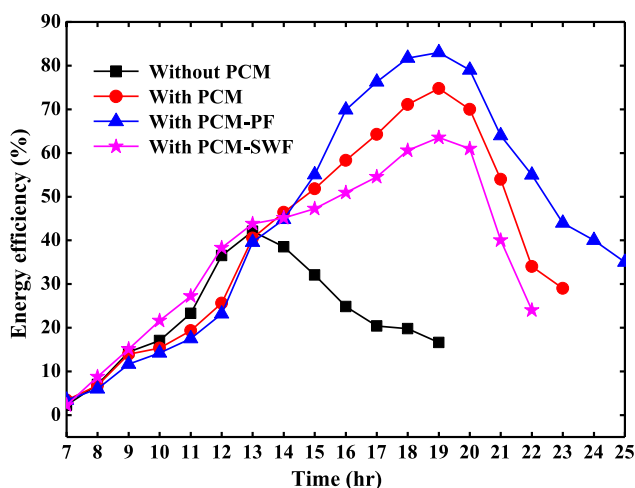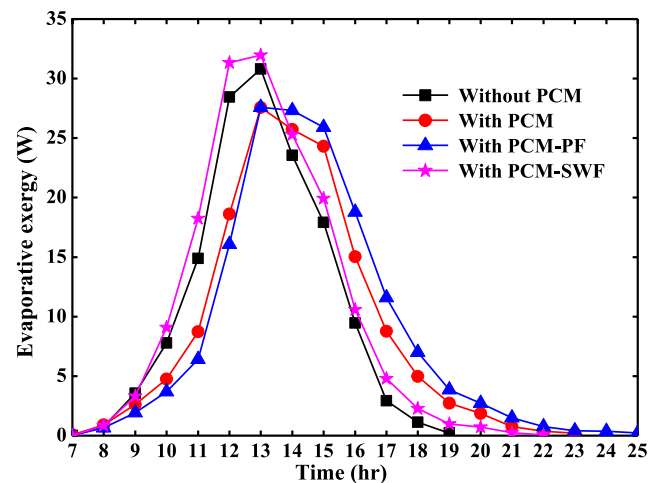Fig. 12 presents the variations of the evaporative exergy rates with

Fig. 12. Hourly evolutions of the evaporative exergy for the studied cases.

time for the studied cases. As seen, as the time progresses, all values show an upward trend until they have peak values around 13:00 PM then, they gradually decline until sunset. Also, it is noted that the evaporative exergy values for all considered cases have the same trend as the trend of brackish water temperatures (see Fig. 8). The evaporative exergy strictly depends on the water temperatures values. As the water temperature rises, the evaporation rate also augments and thus the evaporative exergy enhances. The maximum evaporative exergy for conventional still, still with PCM, still with PCM-PF, and still with PCM-SWF are estimated to be about 31, 28, 27.5, and 32 W, respectively. It is noted that still with PCM-SWF has the maximum evaporative exergy due to the increase of the water temperature in case of using SWF in the basin as stated previously. The figure shows that, during the first half of the day, the evaporative exergy values of solar still with PCM and SWF are greater than the corresponding values of traditional solar still, solar still with PCM, and still with PCM-PF. These results can be explained by the enhanced exposure area of evaporation and increased absorbed radiation due to using SWF. This, in turn, raises the water temperatures in still with PCM-SWF as discussed before in Fig. 8. However, this figure indicates that, during the nighttime, the evaporative exergy in still with PCM-SWF is lower than the corresponding values in still with PCM, and with PCM-PF. This trend is due to the minimization of the wicking property of the steel fibers as the time passes, as previously explained. Thus, a reduction in brackish water temperature is observed that causes lower water evaporation rates. The exergy results show that the total daytime evaporative exergy values for still with PCM-SWF are greater than the corresponding values in conventional still, still with PCM, and still with PCM-PF by approximately 10, 50, and 68%, respectively. Also, the results indicated that total overnight evaporative exergy values for still with PCM-SWF is lower than the corresponding values in cases 2 and 3 by approximately 30 and 55%, respectively. Accordingly, the total daily evaporative exergy for still with PCM-SWF is greater than those of conventional still, still with PCM, and still with PCM-PF by 13, 8, and 2%, respectively. This can be attributed to the significant enhancement in the evaporative exergy rates during sunny hours due to using SWF (positive effect) which is dominant compared to the lower evaporative exergy values at nighttime (negative effect). Hence, it can be concluded that still with PCM-SWF achieved the highest total evaporative exergy rates in comparison with the other tested configurations.

Hourly evolutions of exergetic efficiency for the four considered cases are displayed in Fig. 13. As seen, the figure presents nearly the same trend as the energy efficiency profile (see Fig. 12). The maximum exergy efficiencies for conventional still, still with PCM, still with PCM-PF, and still with PCM-SWF are found to be about 3.14, 32, 47, and 25%, respectively. It was observed that the average exergy efficiency

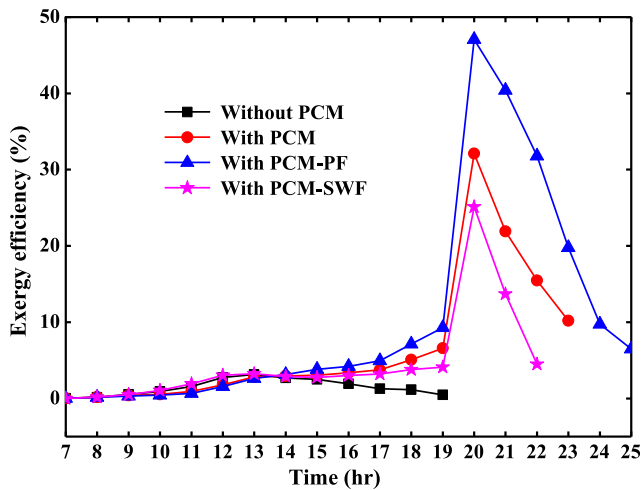Fig. 11. Hourly variations of energy efficiency for the studied cases.

Fig. 13. Hourly variations of exergy efficiency for the studied cases.

values of the solar still with PCM-SWF are greater than the corresponding values of traditional solar still, solar still with PCM and solar still with PCM-PF. Such findings can be attributed to the enhanced evaporative exergy rates of still with PCM-SWF related to other cases, as discussed formerly in Fig. 12. Furthermore, the modified stills (still with PCM, still with PCM-PF, and still with PCM-SWF) exhibited an increment of 5, 12, and 16%, respectively, in terms of average daily exergy efficiency, compared to conventional still. For all the tested cases, the average exergy efficiency for solar still with PCM-SWF is the highest. This is mainly a result of the higher operating water temperature that results in higher evaporative exergy. An interesting observation here is that according to Figs. 10 and 11, the solar still with PCM-PF achieves the highest daily freshwater yield and energy efficiency. Nevertheless, based on the exergetic analysis, the still with PCM-SWF attains the highest exergy efficiency with respect to the other configurations. This outcome can be explained by the substantial enhancement in the evaporative exergy rates during sunny hours due to using SWF in comparison with still with PCM and still with PCM-PF which its evaporative exergy values are drastically affected due to using PCM without SWF. By comparing the exergy efficiency values in this figure with those of energy efficiency in Fig. 11, it can be perceived that the energy efficiency values are significantly greater than the corresponding values of exergy efficiency although they have the same trend. The reason for this result is that exergy analysis signifies the degradation of energy quality and considering the irreversibility in the system processes rather than the concept of conservation of energy. In other words, the high exergy content of solar insolation from the sun (high temperature 6000 K) is significantly degraded to the low temperature of evaporated saline water (low energy quality).

For more analyzing and interpreting the previous results, Table 4 summarizes the overnight and overall daily water productivities of all four tested cases. Also, the average energy and exergy efficiencies of each case are highlighted. Table 4 indicates that still with PCM-PF has the highest overall freshwater productivity and energy efficiency because of the positive effect of using PCM and PF on the still

Table 5
Results of the cost analysis of the studied solar stills.

Type	Conventional	With PCM	With PCM-PF	With PCM-SWF
n (years)	10	10	10	10
i (interest rate%)	0.2	0.2	0.2	0.2
CRF	0.24	0.24	0.24	0.24
P (capital cost $)	190	250	285	252
S	38	50	57	50.4
FAC	45.6	60	68.4	60.5
SSF	0.04	0.04	0.04	0.04
ASV	1.52	2	2.28	2.02
AMC	6.84	9	10.26	9.075
AC	50.9	67	76.4	67.5
P_n (l/m^2 year)	1190.63	1303.8	1390.6	1345
CPL ($/l/m^2)	0.0427	0.051	0.054	0.05

temperatures as stated previously and the conventional still has the lowest values. Also, Table 4 shows that still with PCM-SWF has the highest average exergy efficiency among all tested cases due to utilizing SWF as a porous medium in the basin which has nearly no additional cost to the system as will be shown later in the economic analysis. It is also observed that the average daily solar insolation during all the tested days are close to each other's presented in Table 4.

4.4. Economic analysis

Table 5 shows the outcomes of the economic analysis for the all tested cases of the solar stills. As presented in this table, the conventional solar still represents the most economical still. The reason for this result is that the cost of the solar still only is inexpensive compared to PCM material and even pin fins heat sink. However, the solar still with PCM-SWF is the most economical still compared to other PCM-based solar stills configurations, as depicted in Table 5. This is due to the high freshwater productivity and the cheap cost of the SWF compared to the copper heat sink. Table 5 illustrates that the CPL values for all considered solar stills; traditional one, still with PCM, still with PCM-PF and still with PCM-SWF are computed as 0.0427, 0.051, 0.054 and 0.05 $/l, respectively. By comparing the results of the economic analysis of the tested systems in this work with similar systems in literature, it was reported that the CPL for the simple still [64], still with PCM [28] and still with wick materials [15] was assessed as 0.083, 0.0597 and 0.065 $/l, respectively. These results demonstrated that the CPL values for all solar stills in this study are lower than those reported in the literature, as depicted in Table 5.

5. Conclusions

An experimental performance assessment of solar still system combined with PCM storage unit is energetically, exergetically and economically investigated in this study. Two techniques are used for further enhancing the still performance with PCM which are: embedded copper hollow pin fins (PF) inside the PCM and using mesh steel wool fibers (SWF) in the basin of the solar still with the PCM. Four cases of the solar still are studied and compared in this study, which are: conventional still, still with PCM, still with PCM and PF embedded in the

Table 4
Freshwater productivities, daily solar insolation, energy, and exergy efficiencies.

Solar still system	Without PCM (conventional)	With PCM	With PCM-PF	With PCM-SWF
Tested day	2 Sep. 2017	2 Sep. 2017	4 Sep. 2017	5 Sep. 2017
Total daily radiation (W/m^2 day)	6842	6842	6770	6661
Overnight productivity (kg/m^2)	0.163	0.682	1.0	0.375
Total daily productivity (kg/m^2)	3.262	3.572	3.8094	3.685
Average energy efficiency (%)	31.8	34.8	37.5	36.9
Average exergy efficiency (%)	2.2	2.33	2.49	2.58

PCM, and still with PCM and SWF in the basin. The main conclusions are summarized as follow:

- The total daily accumulative freshwater yields for conventional still, still with PCM, still with PCM-PF, and still with PCM-SWF are approximately 3.26, 3.572, 3.81, and 3.685 kg/m^2, respectively.
- Using SWF in the still basin for PCM based solar still enhances the daytime productivity by 14% with a drop in the overnight productivity by 80%, compared to still with PCM.
- The average energy efficiency of still with PCM-PF is 37.5% which is greater than energy efficiency of conventional still, still with PCM, and still with PCM-SWF by around 17.9, 7.7, and 1.6%.
- The total daily evaporative exergy for still with PCM-SWF is greater than those of conventional still, still with PCM, and still with PCM-PF by 13, 8, and 2%, respectively.
- For all studied cases, the exergy efficiency values are much lower than the energy efficiency.
- Still with PCM-PF achieved the highest accumulated daily water productivity and energy efficiency, however, still with PCM-SWF attained the highest exergy efficiency.
- The costs per liter of freshwater per square meter for the conventional still, still with PCM, still with PCM-PF and still with PCM-SWF are 0.0427, 0.051, 0.054 and 0.05 $/l, respectively.

Acknowledgment

References

[1] Yousef MS, Hassan H, Ahmed M, Ookawara S. Energy and exergy analysis of single slope passive solar still under Egyptian climate conditions. Energy Proc 2017;141:18–23. https://doi.org/10.1016/j.egypro.2017.11.005.

[2] Abdelbar AR, Hassan H, Ookawara S. A numerical study on the effect of the heat sink as condenser on the performance of passive solar still. 5th Int Conf Renew Energy Gener Appl, Al Ain, UAE 2018:256–9.

[3] Fathy M, Hassan H, Salem Ahmed M. Experimental study on the effect of coupling parabolic trough collector with double slope solar still on its performance. Sol Energy 2018;163:54–61. https://doi.org/10.1016/j.solener.2018.01.043.

[4] Mousa H, Gujarathi AM. Modeling and analysis the productivity of solar desalination units with phase change materials. Renew Energy 2016;95:225–32. https://doi.org/10.1016/j.renene.2016.04.013.

[5] Ibrahim AGM, Allam EE, Elshamarka SE. A modified basin type solar still: experimental performance and economic study. Energy 2015;93:335–42. https://doi.org/10.1016/j.energy.2015.09.045.

[6] Al-harahsheh M, Abu-Arabi M, Mousa H, Alzghoul Z. Solar desalination using solar still enhanced by external solar collector and PCM. Appl Therm Eng 2018;128:1030–40. https://doi.org/10.1016/j.applthermaleng.2017.09.073.

[7] Faegh M, Shafii MB. Experimental investigation of a solar still equipped with an external heat storage system using phase change materials and heat pipes. Desalination 2017;409:128–35. https://doi.org/10.1016/j.desal.2017.01.023.

[8] Muftah AF, Alghoul MA, Fudholi A, Abdul-Majeed MM, Sopian K. Factors affecting basin type solar still productivity: a detailed review. Renew Sustain Energy Rev 2014;32:430–47. https://doi.org/10.1016/j.rser.2013.12.052.

[9] Dsilva Winfred Rufuss D, Iniyan S, Suganthi L, Davies PA. Solar stills: a comprehensive review of designs, performance and material advances. Renew Sustain Energy Rev 2016;63:464–96. https://doi.org/10.1016/j.rser.2016.05.068.

[10] Feilizadeh M, Karimi Estahbanati MR, Jafarpur K, Roostaazad R, Feilizadeh M, Taghvaei H. Year-round outdoor experiments on a multi-stage active solar still with different numbers of solar collectors. Appl Energy 2015;152:39–46. https://doi.org/10.1016/j.apenergy.2015.04.084.

[11] Singh DB, Yadav JK, Dwivedi VK, Kumar S, Tiwari GN, Al-Helal IM. Experimental studies of active solar still integrated with two hybrid PVT collectors. Sol Energy 2016;130:207–23. https://doi.org/10.1016/j.solener.2016.02.024.

[12] Singh RV, Kumar S, Hasan MM, Khan ME, Tiwari GN. Performance of a solar still integrated with evacuated tube collector in natural mode. Desalination 2013;318:25–33. https://doi.org/10.1016/j.desal.2013.03.012.

[13] Hassan H, Abo-Elfadl S. Effect of the condenser type and the medium of the saline water on the performance of the solar still in hot climate conditions. Desalination 2017;417:60–8. https://doi.org/10.1016/j.desal.2017.05.014.

[14] Pounraj P, Winston DP, Kabeel AE, Kumar BP, Manokar AM, Sathyamurthy R, et al.

[15] Rashidi S, Rahbar N, Valipour MS, Esfahani JA. Enhancement of solar still by reticular porous media: experimental investigation with exergy and economic analysis. Appl Therm Eng 2018;130:1341–8. https://doi.org/10.1016/j.applthermaleng.2017.11.089.

[16] Shalaby SM, El-Bialy E, El-Sebaii AA. An experimental investigation of a v-corrugated absorber single-basin solar still using PCM. Desalination 2016;398:247–55. https://doi.org/10.1016/j.desal.2016.07.042.

[17] Yeh HM, Chen LC. The effects of climatic, design and operational parameters on the performance of wick-type solar distillers. Energy Convers Manag 1986;26:175–80. https://doi.org/10.1016/0196-8904(86)90052-X.

[18] Nosoko T, Kinjo T, Park CD. Theoretical analysis of a multiple-effect diffusion still producing highly concentrated seawater. Desalination 2005;180:33–45. https://doi.org/10.1016/j.desal.2004.09.031.

[19] Tanaka H, Nakatake Y. Improvement of the tilted wick solar still by using a flat plate reflector. Desalination 2007;216:139–46. https://doi.org/10.1016/j.desal.2006.12.010.

[20] Velmurugan V, Pandiarajan S, Guruparan P, Subramanian LH, Prabaharan CD, Srithar K. Integrated performance of stepped and single basin solar stills with mini solar pond. Desalination 2009;249:902–9. https://doi.org/10.1016/j.desal.2009.06.070.

[21] Huang BJ, Chong TL, Wu PH, Dai HY, Kao YC. Spiral multiple-effect diffusion solar still coupled with vacuum-tube collector and heat pipe. Desalination 2015;362:74–83. https://doi.org/10.1016/j.desal.2015.02.011.

[22] Omara ZM, Kabeel AE, Essa FA. Effect of using nanofluids and providing vacuum on the yield of corrugated wick solar still. Energy Convers Manag 2015;103:965–72. https://doi.org/10.1016/j.enconman.2015.07.035.

[23] Mettawee EBS, Assassa GMR. Experimental study of a compact PCM solar collector. Energy 2006;31:2622–32. https://doi.org/10.1016/j.energy.2005.11.019.

[24] Al-Kayiem HH, Lin SC. Performance evaluation of a solar water heater integrated with a PCM nanocomposite TES at various inclinations. Sol Energy 2014;109:82–92. https://doi.org/10.1016/j.solener.2014.08.021.

[25] Fath HES. Technical assessment of solar thermal energy storage technologies. Renew Energy 1998;14:35–40. https://doi.org/10.1016/S0960-1481(98)00044-5.

[26] El-Sebaii AA, Al-Ghamdi AA, Al-Hazmi FS, Faidah AS. Thermal performance of a single basin solar still with PCM as a storage medium. Appl Energy 2009;86:1187–95. https://doi.org/10.1016/j.apenergy.2008.10.014.

[27] Dashtban M, Tabrizi FF. Thermal analysis of a weir-type cascade solar still integrated with PCM storage. Desalination 2011;279:415–22. https://doi.org/10.1016/j.desal.2011.06.044.

[28] Ansari O, Asbik M, Bah A, Arbaoui A, Khmou A. Desalination of the brackish water using a passive solar still with a heat energy storage system. Desalination 2013;324:10–20. https://doi.org/10.1016/j.desal.2013.05.017.

[29] Arunkumar T, Denkenberger D, Ahsan A, Jayaprakash R. The augmentation of distillate yield by using concentrator coupled solar still with phase change material. Desalination 2013;314:189–92. https://doi.org/10.1016/j.desal.2013.01.018.

[30] Arunkumar T, Kabeel AE. Effect of phase change material on concentric circular tubular solar still-Integration meets enhancement. Desalination 2017;414:46–50. https://doi.org/10.1016/j.desal.2017.03.035.

[31] Bazri S, Badruddin IA, Naghavi MS, Bahiraei M. A review of numerical studies on solar collectors integrated with latent heat storage systems employing fins or nanoparticles. Renew Energy 2018;118:761–78. https://doi.org/10.1016/j.renene.2017.11.030.

[32] Hawlader MNA, Uddin MS, Khin MM. Microencapsulated PCM thermal-energy storage system. Appl Energy 2003;74:195–202. https://doi.org/10.1016/S0306-2619(02)00146-0.

[33] Khodadadi JM, Hosseinizadeh SF. Nanoparticle-enhanced phase change materials (NEPCM) with great potential for improved thermal energy storage. Int Commun Heat Mass Transf 2007;34:534–43. https://doi.org/10.1016/j.icheatmasstransfer.2007.02.005.

[34] Zhao CY, Lu W, Tian Y. Heat transfer enhancement for thermal energy storage using metal foams embedded within phase change materials (PCMs). Sol Energy 2010;84:1402–12. https://doi.org/10.1016/j.solener.2010.04.022.

[35] Frusteri F, Leonardi V, Vasta S, Restuccia G. Thermal conductivity measurement of a PCM based storage system containing carbon fibers. Appl Therm Eng 2005;25:1623–33. https://doi.org/10.1016/j.applthermaleng.2004.10.007.

[36] Reddy KS. Thermal modeling of PCM-based solar integrated collector storage water heating system. J Sol Energy Eng 2007;129:458. https://doi.org/10.1115/1.2770753.

[37] Sharshir SW, Peng G, Yang N, Eltawil MA, Ali MKA, Kabeel AE. A hybrid desalination system using humidification-dehumidification and solar stills integrated with evacuated solar water heater. Energy Convers Manag 2016;124:287–96. https://doi.org/10.1016/j.enconman.2016.07.028.

[38] Sahota L, Shyam, Tiwari GN. Analytical characteristic equation of nanofluid loaded active double slope solar still coupled with helically coiled heat exchanger. Energy Convers Manag 2017;135:308–26. https://doi.org/10.1016/j.enconman.2016.12.078.

[39] Beemkumar N, Karthikeyan A, Yuvarajan D, Lakshmi Sankar S. Experimental investigation on improving the heat transfer of cascaded thermal storage system using different fins. Arab J Sci Eng 2017;42:2055–65. https://doi.org/10.1007/s13369-017-2455-9.

[40] Al-Abidi AA, Mat S, Sopian K, Sulaiman MY, Mohammad AT. Internal and external fin heat transfer enhancement technique for latent heat thermal energy storage in triplex tube heat exchangers. Appl Therm Eng 2013;53:147–56. https://doi.org/10.

1016/j.applthermaleng.2013.01.011.

[41] Murali G, Mayilsamy K. Effect of circular fins on latent heat storage to enhance solar water heater, an experimental study. Appl Mech Mater 2015;787:13–7. https://doi.org/10.4028/www.scientific.net/AMM.787.13.

[42] Waqas A, Jie J, Xu L. Thermal behavior of a PV panel integrated with PCM-filled metallic tubes: an experimental study. J Renew Sustain Energy 2017;9. https://doi.org/10.1063/1.4995022.

[43] Ranjan KR, Kaushik SC, Panwar NL. Energy and exergy analysis of passive solar distillation systems. Int J Low-Carbon Technol 2016;11:211–21. https://doi.org/10.1093/ijlct/ctt069.

[44] Aghaei Zoori H, Farshchi Tabrizi F, Sarhaddi F, Heshmatnezhad F. Comparison between energy and exergy efficiencies in a weir type cascade solar still. Desalination 2013;325:113–21. https://doi.org/10.1016/j.desal.2013.07.004.

[45] Shanmugan S, Manikandan V, Shanmugasundaram K, Janarathanan B, Chandrasekaran J. Energy and exergy analysis of single slope single basin solar still. Int J Ambient Energy 2012;33:142–51. https://doi.org/10.1080/01430750.2012.686194.

[46] Torchia-Núñez JC, Porta-Gándara MA, Cervantes-de Gortari JG. Exergy analysis of a passive solar still. Renew Energy 2008;33:608–16. https://doi.org/10.1016/j.renene.2007.04.001.

[47] Vaithilingam S, Esakkimuthu GS. Energy and exergy analysis of single slope passive solar still: an experimental investigation. Desalin Water Treat 2014;55:1433–44. https://doi.org/10.1080/19443994.2014.928794.

[48] Deniz E. Energy and exergy analysis of flat plate solar collector-assisted active solar distillation system. Desalin Water Treat 2016;57:24313–21. https://doi.org/10.1080/19443994.2016.1143402.

[49] Kianifar A, Zeinali Heris S, Mahian O. Exergy and economic analysis of a pyramid-shaped solar water purification system: active and passive cases. Energy 2012;38:31–6. https://doi.org/10.1016/j.energy.2011.12.046.

[50] Asbik M, Ansari O, Bah A, Zari N, Mimet A, El-Ghetany H. Exergy analysis of solar desalination still combined with heat storage system using phase change material (PCM). Desalination 2016;381:26–37. https://doi.org/10.1016/j.desal.2015.11.031.

[51] Sarhaddi F, Farshchi Tabrizi F, Aghaei Zoori H, Mousavi SAHS. Comparative study of two weir type cascade solar stills with and without PCM storage using energy and exergy analysis. Energy Convers Manag 2017;133:97–109. https://doi.org/10.1016/j.enconman.2016.11.044.

[52] Singh DB, Tiwari GN. Exergoeconomic, enviroeconomic and productivity analyses

[53] Jegadheeswaran S, Pohekar SD, Kousksou T. Exergy based performance evaluation of latent heat thermal storage system: a review. Renew Sustain Energy Rev 2010;14:2580–95. https://doi.org/10.1016/j.rser.2010.07.051.

[54] Li G. Energy and exergy performance assessments for latent heat thermal energy storage systems. Renew Sustain Energy Rev 2015;51:926–54. https://doi.org/10.1016/j.rser.2015.06.052.

[55] Kabeel AE, Abdelgaied M. Improving the performance of solar still by using PCM as a thermal storage medium under Egyptian conditions. Desalination 2016;383:22–8. https://doi.org/10.1016/j.desal.2016.01.006.

[56] Tillack MS, Raffray AR, Pulsifer JE. Improved performance of energy recovery ventilators using advanced heat transfer. Media 2001:44. https://doi.org/10.1002/ejoc.201200111.

[57] Turkoglu M, Baba A, Ozcan H. Determination and evaluation of some physi-cochernical parameters in the Dardanelles (Canakkale Strait, Turkey) using multiple probe system and geographic information system. Nord Hydrol 2006;37:293–301. https://doi.org/10.2166/nh.2006.012.

[58] Abdel-Halim AM, Aly-Eldeen MA. Characteristics of mediterranean sea water in vicinity of Sidikerir region, west of Alexandria, Egypt. Egypt J Aquat Res 2016;42:133–40. https://doi.org/10.1016/j.ejar.2016.05.002.

[59] Taylor JR. An introduction to error analysis: the study of uncertainties in physical measurements. University Science Books; 1997.

[60] Petela R. Exergy of undiluted thermal radiation. Sol Energy 2003;74:469–88. https://doi.org/10.1016/S0038-092X(03)00226-3.

[61] Deniz E, Çınar S. Energy, exergy, economic and environmental (4E) analysis of a solar desalination system with humidification-dehumidification. Energy Convers Manag 2016;126:12–9. https://doi.org/10.1016/j.enconman.2016.07.064.

[62] Tiwari GN, Sahota L. Review on the energy and economic efficiencies of passive and active solar distillation systems. Desalination 2017;401:151–79. https://doi.org/10.1016/j.desal.2016.08.023.

[63] Esfahani JA, Rahbar N, Lavvaf M. Utilization of thermoelectric cooling in a portable active solar still – an experimental study on winter days. Desalination 2011;269:198–205. https://doi.org/10.1016/j.desal.2010.10.062.

[64] Kabeel AE. Performance of solar still with a concave wick evaporation surface. Energy 2009;34:1504–9. https://doi.org/10.1016/j.energy.2009.06.050.